Numerical simulation of the response of Li state densities to power interruption in an inductively coupled plasma

Spectrochimica Acta, Vol. 48B, No. 13, pp. 1579–1592, 1993
Printed in Great Britain.

0584–8547/93 $6.00 + .00

Numerical simulation of the response of Li state densities to power interruption in an inductively coupled plasma

F. H. A. G. Fey, D. A. Benoy, J. M. de Regt, J. A. M. van der Mullen and D. C. Schram

Physics Department, Eindhoven University of Technology, P.O. Box 513, 5600 MB Eindhoven, The Netherlands

(*Received* 17 *November* 1992; *accepted* 20 *August* 1993)

Abstract—The response of Li levels to power interruption in an inductively coupled plasma (ICP) is calculated by using a time dependent collisional radiative model of the Li system, extended with transport. The input data for the calculations, the electron density, the electron temperature, the transport frequency of the ions and the evaporation source are estimated on the basis of experiments. The obtained results show a very good agreement with experimental results when the ionization flow through the system by evaporation and heating of analyte is taken into account.

1. Introduction

In previous articles [1, 2] devoted to the experimental study of the response of line emission to the interruption of the power of an inductively coupled plasma (ICP), it was found that the character of the analyte emission response was essentially different from that of the levels of the main argon gas, and that this character was a very sensitive function of the flow rates, the power and the plasma position [1].

Since this analyte response might be based on the same phenomena that are responsible for the analytical resolving power of the ICP, it is important to study the observed experimental behaviour theoretically. This might improve our insight into and understanding of the essential features of the ICP.

Our strategy in this theoretical approach has a two-fold structure. First (the aim of the present paper), a time dependent collisional radiative (CR) model will be constructed describing the temporal behaviour of lithium levels for given temporal dependencies of the electron temperature T_e, heavy particle temperature T_h, electron density, and the transport coefficient ν_t^+ of the lithium ion. Second (the subject of a forthcoming paper), a fluid model for the spatial and temporal behaviour of T_e, T_h, n_e and ν_t^+, will be proposed. So, with the use of the CR-model the temporal behaviour of Li emission during the power interruption can be described as a function of time and of spatial position.

Collisional radiative models are used to describe the effect of the sources of departure from equilibrium [3, 4] on the atomic state distribution function (ASDF), or, to state it differently, to compute the density of excited levels of atoms and/or ions and the ionization and recombination coefficients under non-LTE conditions. The CR model as constructed in the present paper has some differences with respect to those already published by Hasegawa and Haraguchi [5] and Bacri and Gomes [6], as detailed below.

First, we will use a cut-off technique by which the number of excited levels can be reduced drastically and thus improve the accuracy of the stepwise ionization or recombination flow in the system.

Second, the present model is time dependent by which it is capable to follow the temporal behaviour of excited levels during the interruption of the power.

Third, apart from the escape of radiation being the only source of departure from the ASDF equilibrium in Refs [5, 6] we will study the effect of particle transport as well. It is found that this phenomenon, characterized by ν_t^+, the ion transport frequency of Li ions, and the evaporation source, S^{evap}, of ground level atoms, has a large effect

on the shape of the ASDF. This can be understood globally, by realizing that owing to the evaporation of droplets, ground level atoms are produced with a rate that may be so large that it considerably exceeds the ionization. As a consequence, the Saha balance of ionization and recombination will be distorted and the ground level will be overpopulated with respect to the Saha density as prescribed by the values of n_e, T_e and n_+ (ion density). This overpopulation can be characterized using the parameter $b(1) = n(1)/n^S(1)$, i.e. the ratio of the actual value of $n(1)$ and the value as prescribed by the Saha formula. In agreement with Refs [3, 4], it is found in this study that this ground level overpopulation propagates within the system to higher excited levels causing a departure of the ASDF from its equilibrium Boltzmann–Saha value. This effect of transport on the ASDF explains why so many different values are reported in the literature for the excitation temperature of analytes, and why the corresponding 2λ temperature determination is strongly dependent on the selected couple of lines.

2. The Structure of a Time Dependent Collisional Radiative Model

To evaluate the temporal behaviour of an element level p, the set of coupled continuity equations

$$\frac{\partial n_p}{\partial t} + \nabla \cdot (n_p w_p) = S_p^{CR} + S_p^{evap} \tag{1}$$

for all the levels involved, has to be solved. In this equation, n_p represents the number density of atoms in level p, w_p is the mean velocity, S_p^{CR} is the source term due to collisional and radiative processes and S_p^{evap} is the source term due to evaporation. Since we will assume that evaporation leads to production of ground level atoms, only S_1^{evap} will be non-zero.

For excited levels, the frequencies of collisional and radiative population and depopulation processes are very high, compared to those of transport processes. This means that Sp_p^{CR} (equal to Production(p) − Destruction(p)) consists of positive (i.e. production) and negative (i.e. destruction) terms that almost cancel each other. The difference between destruction and production is much smaller than production and destruction separately, so that we may state that Production(p) − Destruction(p) ≈ 0, or $S_p^{CR} \approx 0$. Therefore, the excited levels can be considered to be in a quasi-steady state (QSS), which is only determined by the main particle reservoirs, the ground levels of the atom (n_1) and the ion (n_+) of that element, and the parameters that govern the population balances (T_e and n_e). The temporal behaviour of the excited levels is therefore determined by the changes in n_1, n_+, T_e and n_e.

Therefore, Eqn 1 can be simplified, giving:

$$\text{ground level:} \quad \frac{\partial n_1}{\partial t} + \nabla \cdot (n_1 w_1) = S_1^{CR} + S_1^{evap}; \tag{2}$$

$$\text{excited levels:} \quad 0 = S_p^{CR}; \tag{3}$$

$$\text{ion level:} \quad \frac{\partial n_+}{\partial t} + \nabla \cdot (n_+ w_+) = S_+^{CR}. \tag{4}$$

For reasons of simplicity, the transport term for ions will be written down by means of a transport frequency, ν_t^+, defined by:

$$\nabla \cdot (n_+ w_+) = \nu_t^+ n_+. \tag{5}$$

Since the sum of the CR-terms, S_p^{CR}, over all the levels must cancel and the fact that these terms equal zero for excited levels, it must yield $S_1^{CR} = -S_+^{CR}$. It can also be shown [3] that in the steady state S_+^{CR} can be written as:

$$S_+^{CR} = n_e n_1 K_{CR} - n_e n_+ \alpha_{CR} \tag{6}$$

in which K_{CR} represents the total ionization coefficient from ground level atoms and α_{CR} the total recombination coefficient of ions. The terms $n_e n_1 K_{CR}$ and $n_e n_+ \alpha_{CR}$ can be interpreted as, respectively, the effective ionization flow and the recombination flow, while $n_e n_1 K_{CR} - n_e n_+ \alpha_{CR}$ is the net ionization flow. A negative value represents a recombining system.

For a proper description of the power interruption-induced behaviour of the occupation of an excited level, we must know (1) the value of S_1^{evap} and ν_t^+, (2) the dependence of K_{CR}, α_{CR} and the various terms in S_p^{CR} on n_e and T_e, and (3) the temporal behaviour of n_e and T_e during the power interruption.

Anticipating a forthcoming article, Section 3 gives an estimation of ν_t^+. Section 4 describes K_{CR}, α_{CR} and the terms S_p^{CR} using a CR-model with a numerical bottom and analytical top. The temporal behaviour of n_e and T_e and the consequences on the various elementary processes are given in Section 5.

3. The Transport of Ions and Ground Level Atoms

The study of the transport associated with the main particle reservoirs n_1 and n_+ is closely connected to the phenomena around the evaporating analytes. The evaporated analyte leaving the particulate has a low temperature, which is just slightly higher than the temperature of the particulate. While the analyte diffuses away from the droplets it gets heated and if the temperature is high enough excited analytes will be created that will emit radiation. This region around the particle will be termed here "aurora". The diameter of the aurora, which depends on transport coefficients, is an important parameter. It is clear that, if the diameter is large compared to the interdroplet distance (aurora overlap), the diffusion of analytes essentially differs from the case of separate auroras.

3.1. *The separate aurora model*

Consider a single particle imbedded in a hot plasma. For a spectro-analytical ICP this is a polluted water droplet; for a plasma spraying application, the particulate might be metallic. Owing to heat transfer from the plasma, evaporation takes place creating a cloud of atoms that initially are in the ground level. As a consequence of the electron–atom collisions (stepwise), ionization will take place. The ions formed will diffuse into the plasma with a flux given by:

$$n_t^+ w_+ = -D \nabla n_+ \tag{7}$$

in which D is the ambipolar diffusion coefficient. The term $n_+ w_+$ represents the ion flux per unit of area moving away from the particle, which, expressed per unit of volume, gives the divergence

$$\nabla \cdot (n_+ w_+) = -\nabla \cdot D \nabla n_+ . \tag{8}$$

Using Eqn 5 we get an approximation

$$\nu_t^+ \simeq \frac{D}{\Lambda^2} \tag{9}$$

for the frequency at which created ions are transported outward. Here, Λ is the gradient length in the aurora. To estimate the frequency, we take $\Lambda = 30$ μm, a value between the radius (5–10 μm) and the interdroplet distance (100 μm). Using for the ambipolar diffusion coefficient a typical value of $D \simeq 10^{-3}$ ms^{-2} [7], we find a value of $\nu_t^+ = 10^6$ s^{-1}.

This simple model is only applicable to those conditions where the electron

temperature is so high that the ionization of atoms takes place immediately after evaporation. This can be found for a metallic particle in a spraying plasma or in an ICP into which desolvated droplets are injected. The fact that under those conditions the transport of ions with a frequency of $\nu_t^+ = 10^6\ s^{-1}$ is much larger than the recombination frequency (typically $n_e\alpha_{CR} = 10^3\ s^{-1}$) will disturb the Saha balance, which results in an overpopulation of the ground level, propagating through the system.

3.2. *The aurora overlap model*

The conditions in an analytical ICP used in combination with a cross-flow nebulizer are not well described by the separate aurora model. The reason is that the droplets entering the central channel will have a relatively moderate temperature increase tempered by the latent heat of H_2O evaporation and dissociation. By these processes, the relatively slow temperature increase results in a spatial separation of evaporation, dissociation of H_2O and the evaporation and ionization of the analyte. So, before ionization takes place, the vapour clouds associated with adjacent droplets have been merged into each other. However, immediately after the energy drain caused by the dissociation (at about 0.3 eV) of H_2O, the temperature in the central channel will increase relatively quickly so that the ionization degree of analytes around 0.4 eV is increased accordingly. From this description, it can be concluded that besides the evaporation source, the increase of T_e also contributes to flow through the analyte system.

A value for the transport frequency can also be derived by estimating the ion density gradient length to be 1 mm. Together with an axial velocity in the order of 10 ms^{-1}, these estimates lead to:

$$\nu_t^+ \simeq w\frac{\nabla \cdot n_+}{n_+} \simeq 10\frac{n_+}{10^{-3}n_+} = 10^4\ s^{-1}. \tag{10}$$

In the subsequent sections we will select the following values for the ion transport coefficient: (1) $\nu_t^+ = 0\ s^{-1}$; (2) $\nu_t^+ = 10^4\ s^{-1}$; and (3) $\nu_t^+ = 10^6\ s^{-1}$. This covers the whole regime of plasma regions without outward transport and the aurora overlap transport up to the separate aurora model. The evaporation source, S^{evap}, is in any case selected in such a way that the outward transport of ions is fed by ground level atoms created by evaporation.

4. Collisional Radiative Model

A collisional radiative model (CRM) describes the collisional and radiative production and destruction processes of a level p. We will take into account the collisional excitation and de-excitation (Boltzmann processes, B), collisional ionization and recombination (Saha processes, S), radiative recombination and radiative decay. It is justified to assume that the plasma is optically thin for Li transitions, so that the inverse process of emission absorption, may be neglected. In the model, the lowest level is the atomic ground level and the highest the ionic ground level. Since Li^+ has a He-like configuration, excitation in the ionic system can be neglected.

Therefore, the source term for atomic levels reads:

$$(1 \le p):\ S_p^{CR} = n_e \sum_{q\neq p} n_q k_{qp} - n_e n_p \sum_{q\neq p} k_{pq} + \sum_{q>p} n_q A_{qp} - n_p \sum_{q<p} A_{pq} + n_e n_+ (n_e k_{+p} + A_{+p}) - n_e n_p k_{p+}$$

whereas the ionic ground level is described by:

$$S_+^{CR} = n_e \sum_q n_q k_{q+} - n_e^2 n_+ \sum_q k_{+q} - n_e n_+ \sum_q A_{+q}. \tag{11}$$

Table 1. Overview of the levels of Li [9]; note that some levels are coalesced

Level	Statistical weight	Excitation energy (eV)
2*s*	2	0.000
2*p*	6	1.847
3*s*	2	3.372
3*p*	6	3.833
3*d*	10	3.877
4*s*	2	4.340
4*p*	6	4.520
4*d*&4*f*	24	4.540
5*s*	2	4.747
5*p*	6	4.836
5*d*&5*f*&5*g*	42	4.846
6 total	72	5.007
ion	1	5.390

In these equations, k represents the T_e-dependent rate coefficient for electron collision processes. These are calculated by using the semi-empirical formulae of VRIENS and SMEETS [8]. The A values represent the transition probabilities for radiative processes [9]. The subscripts indicate the initial and the final level of the process. To reduce the number of excited levels drastically, a method for treating the highly excited levels analytically is used. This method, introduced by VAN DER MULLEN [3, 4], was applied recently by BENOY *et al.* [10] for the Ar I system. It is based on the fact that high in the atomic system (roughly estimated, for all levels where the ionization energy, I_p, is smaller than the average energy of the electrons, i.e. $I_p < kT_e$), stepwise collisional processes are favoured over "jumping" processes. An additional demand for this approach is that the levels should be collisionally dominated.

5. NUMERICAL RESULTS

5.1. *Calculations for steady state situations*

First, we will discuss steady state calculations, which are a special case of Eqns (2)–(4). The input parameters are the atomic data, given in Tables 1–3, and the plasma parameters n_e, T_e and ν_t^+. The output parameters are α_{CR}, K_{CR} and the level densities, which are scaled to the total density of the analyte. In Fig. 1(a), the results

Table 2. Overview of the transition probabilities in Li [9]

Initial level	Final level	A-value (s^{-1})	Initial level	Final level	A-value (s^{-1})
2*p*	2*s*	3.72×10^7	4*d*	3*p*	6.85×10^6
3*p*	2*s*	1.17×10^6	5*d*	3*p*	3.41×10^6
4*p*	2*s*	1.42×10^6	4*p*	3*d*	5.52×10^5
5*p*	2*s*	1.07×10^6	5*p*	3*d*	2.31×10^5
3*s*	2*p*	3.49×10^7	4*f*	3*d*	1.38×10^7
4*s*	2*p*	1.01×10^7	5*f*	3*d*	4.63×10^6
5*s*	2*p*	4.60×10^6	4*p*	4*s*	7.72×10^5
3*d*	2*p*	7.16×10^7	5*s*	4*p*	2.25×10^6
4*d*	2*p*	2.30×10^7	5*d*	4*p*	1.36×10^6
5*d*	2*p*	1.06×10^7	5*p*	4*d*	2.86×10^5
3*p*	3*s*	3.77×10^6	5*f*	4*d*	2.58×10^6
4*s*	3*p*	7.46×10^6	5*p*	5*s*	2.33×10^5
5*s*	3*p*	2.76×10^6			

Table 3. Overview of oscillator strengths in Li [9]

Initial level	Final level	Oscillator strength	Initial level	Final level	Oscillator strength
2*s*	2*p*	0.753	3*d*	4*p*	0.0184
2*s*	3*s*	0.001	3*d*	4*d*&4*f*	1.01
2*s*	3*p*	0.0055	4*s*	4*p*	0.001
2*p*	3*s*	0.115	4*s*	5*s*	0.001
2*p*	3*p*	0.001	4*s*	5*p*	0.001
2*p*	3*d*	0.667	4*p*	4*d*&4*f*	0.135
3*s*	3*p*	0.001	4*p*	5*s*	0.355
3*s*	4*s*	0.001	4*p*	5*p*	0.001
3*s*	4*p*	0.001	4*p*	5*d*&5*f*&5*g*	0.494
3*p*	3*d*	0.001	4*d*	5*p*	0.045
3*p*	4*s*	0.223	4*d*&4*f*	5*d*&5*f*&5*g*	0.878
3*p*	4*p*	0.001	5*s*	5*p*	2.05
3*p*	4*d*&4*f*	0.527	5*p*	5*d*&5*f*&5*g*	0.19

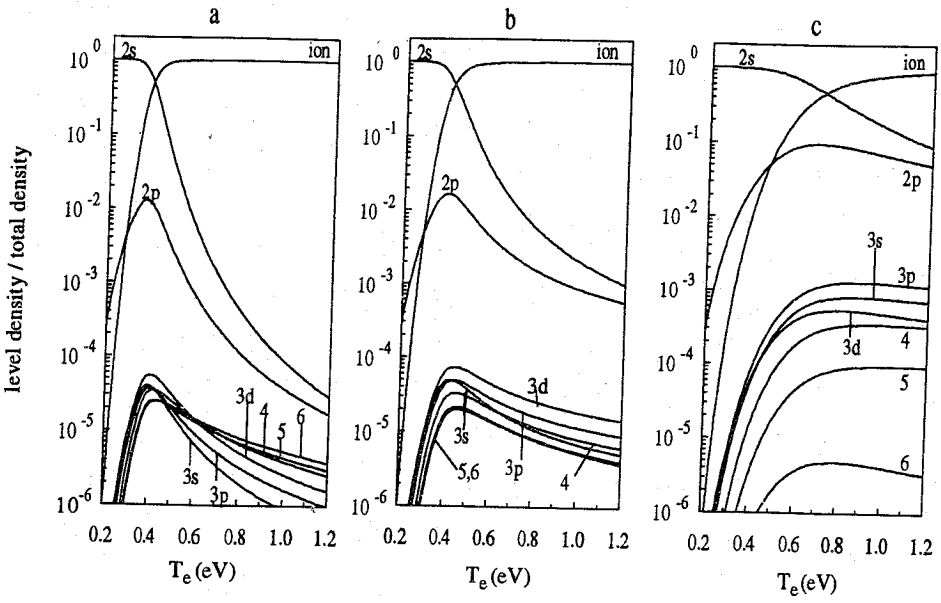

Fig. 1. Steady state densities of the various levels as a function of T_e; $n_e = 3 \times 10^{20}$ m^{-3} and values of $\nu_t^+ = -(\nabla\cdot(n_1 w_1) + S_1^{evap})/n_+$ are (a) 0, (b) 10^4 and (c) 10^6 s^{-1}.

are shown as a function of T_e for $n_e = 3 \times 10^{20}$ m^{-3} and $\nu_t^+ = 0$ s^{-1}. At low T_e values, a small ion density is observed, while the ground level density is, as might be expected, large. At higher temperatures, the ground level density decreases and the ion density increases. At approximately 0.4 eV, the ion density equals the ground level density. The excited levels show a rather different temperature dependence, characterized by a sharp increase, with T_e showing a maximum at approximately 0.4 eV. Above that T_e value, the densities of the excited levels decrease with T_e. Note that this fact already provides a possibility of explaining the different behaviours of the Li line intensities when power interruption occurs. When the initial T_e is above a critical value, in this case approximately 0.4 eV, the intensity after cooling will be higher than before, whereas that intensity will be lower when the initial T_e is lower than the critical value. The information in this figure can also be used to give an indication of transport through the system. Suppose the velocity of the plasma in the centre is of the order of 10 ms^{-1}, that T_e increases 0.025 eV mm^{-1}, that T_e equals 0.4 eV at position A and that no new analyte atoms are formed. At a position 1 mm

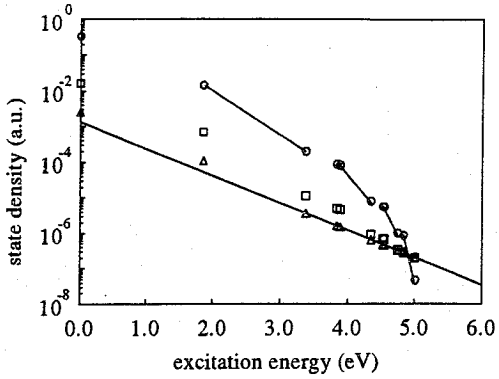

Fig. 2. The results for three computed ASDFs using the CR model for $n_e = 3 \times 10^{20}$ m^{-3} and $T_e = 0.6$ eV: Δ denotes $\nu_t^+ = 0$ s^{-1}; $\square$, $\nu_t^+ = 10^4$ s^{-1}; $\bigcirc$, $\nu_t^+ = 10^6$ s^{-1}. The solid line segments show that the slope, i.e. $T_{2\lambda}$, is not constant.

downstream from position A, the relative density of ions has increased 30% compared to the value at A, according to the results presented in Fig. 1(a). Using Eqn 10, this leads to a value of $\nu_t^+ = 3 \times 10^3$ s^{-1} in this small interval. Of course this result is not very accurate since no transport was assumed in the calculations, but it gives at least an indication of the importance of temperature increase along the central channel.

When the calculation is repeated for $\nu_t^+ = 10^4$ s^{-1} and $\nu_t^+ = 10^6$ s^{-1}, Fig. 1(b) and (c) are obtained. They have globally the same shape as Fig. 1(a), but the T_e-dependence is much smoother and the temperature at which the ground level density decreases is much larger than in the case of $\nu_t^+ = 0$ s^{-1}.

In Fig. 2, Boltzmann plots of the ASDF in the Li system are shown for $T_e = 0.6$ eV. Note that the ASDF generated for large ν_t^+ values gives in a Boltzmann plot ($\log \eta(p)$ vs E) a variable slope (cf. Fig. 2). The "temperature" deduced from this slope has nothing to do with the electron temperature. Therefore, the large transport provides an explanation for the well known fact that $T_{2\lambda}$ depends on the selected wavelengths, i.e. upper levels. In fact, in systems where the overpopulation of the ground level is large and in which stepwise excitation is dominant, the ASDF does not obey the Boltzmann distribution law, and according to VAN DER MULLEN [3], the overpopulation factor to the Saha density $b(p)$ of a highly excited level (for which yields $kT_e < I_p/3$) should be in the order of:

$$b(p) = 1 + b_0 p_{\text{eff}}^{-6} \tag{12}$$

where p_{eff} is the effective principal quantum number, given by $p_{\text{eff}} = (13.6/I_p)^{\frac{1}{2}}$ and b_0 is a reference overpopulation that depends on input parameters like ν_t^+ and the transition probabilities. It is shown in Fig. 3 that Eqn 12 gives a much better description than the Boltzmann plot in the cases of $\nu_t^+ = 10^4$ s^{-1} and $\nu_t^+ = 10^6$ s^{-1}.

It is instructive to compare the effect of particle transport on the ASDF with that of photon transport. Both phenomena are processes that are not compensated for by inverse processes, i.e. the lack of absorption does not compensate emission and the lack of inward transport of ions does not compensate the outward flux. In both situations, this will disturb the electron induced balances of Boltzmann (excitation vs de-excitation) and Saha (ionization vs recombination); a steady state situation can only be realized if excitation prevails over de-excitation (and ionization over recombination). This comparison is elucidated in Fig. 4 for two simple systems; in the first system (A), radiative recombination of ions is not cancelled by absorption and in the second system (B), ground level atoms are transported into the system while ions are removed (under steady state conditions it must be supported by a net ionization flow of magnitude $\nu_t^+ n_+$ through the system). The systems are mathematically equivalent if $A_{+p} = \nu_t^+$, but, owing to physical properties, the frequency ν_t^+ in system

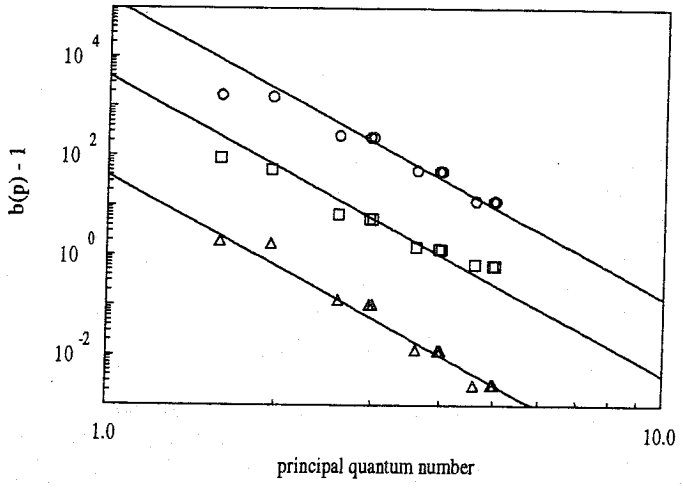

Fig. 3. The same results of three computed ASDFs as given in Fig. 2 but now presented in a $\log(b - 1)$ vs $\log(p_{eff})$ graph. It is shown that the p_{eff}^{-6} behaviour, as predicted in Ref. [3], gives a good description.

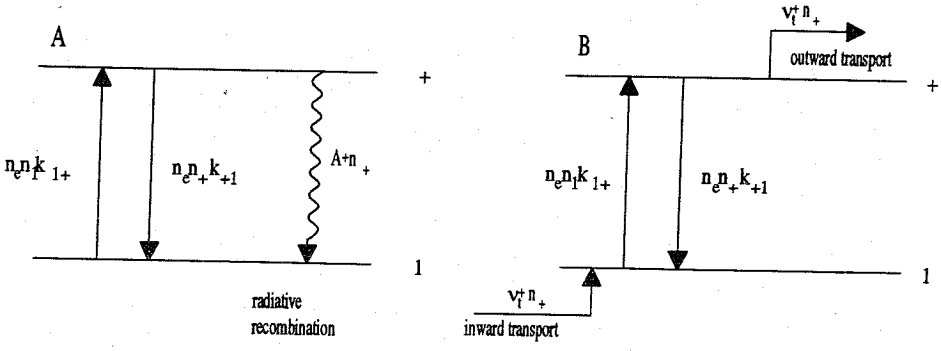

Fig. 4. Two systems that create overpopulation of the ground level. In case A, ions recombine by radiation to the ground level with a rate of n^+A^+, while in case B, ions are removed with a rate of $n^+\nu_t^+$ and a same number rate is introduced into the plasma as ground level atoms. Although the ionization and recombination owing to collisions would create LSE, the unbalanced processes prohibit the system from reaching LSE. Note that the systems are mathematically equivalent if $\nu_t^+ = A^+$.

B can have much larger values than A_{+p} in case A. The results of Hasegawa and Haraguchi [5] and Bacri and Gomes [6] correspond to system A, or, which is the same, our results for the case $\nu_t^+ = 0\ s^{-1}$.

As a next step in the study of the results of the CR model, we will investigate the ratio n_1/n_+ as shown, in Fig. 5(a). The considered n_e range can be divided into three regions:

(a) *A region of low* n_e *values below* $n_e \approx 5 \times 10^{17}\ m^{-3}$. In this interval, the electron density is so small that stepwise excitation is almost blocked, so that ionization processes are only caused by direct ionization. When no transport is assumed (case 1 in Fig. 5) then direct ionization is equilibrated by direct stepwise radiative recombination. This balance is known as the corona balance, which can be expressed mathematically by:

$$n_e n_1 K_{1+} = n_e n_+ \alpha_{CR}. \tag{13}$$

This is equivalent to:

$$\frac{n_1}{n_+} = \frac{\alpha_{CR}}{K_{1+}}. \tag{14}$$

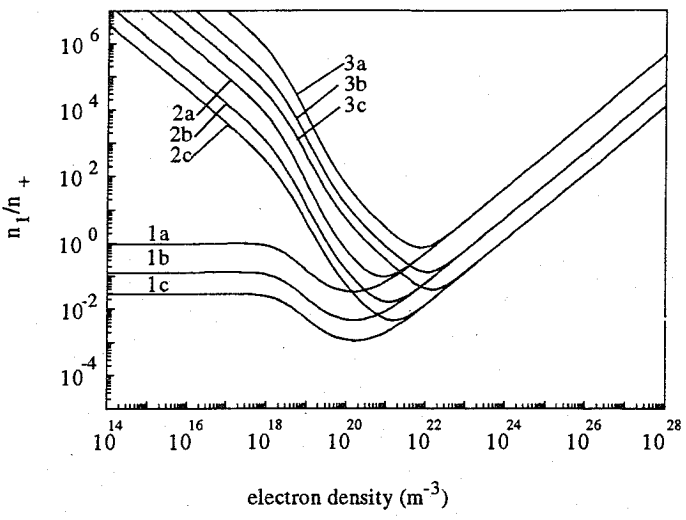

Fig. 5. The steady state ratio n_1/n_+ as a function of the electron density for T_e: (a) 0.5 eV; (b) 0.6 eV; and (c) 0.7 eV; and ν_t^+: (1) 0 s^{-1}; (2) 10^4 s^{-1}; and (3) 10^6 s^{-1}.

Note that n_1/n_+ is independent of n_e in this situation, which is indeed shown in Fig. 5(a). In the case of a large transport rate of ions (cases 2 and 3 in Fig. 5) the produced ions are removed by the transport so that the equation for this situation is:

$$n_e n_1 K_{1+} = n_+ \nu_t^+ \tag{15}$$

or written in terms of n_1/n_+

$$\frac{n_1}{n_+} = \frac{\nu_t^+}{n_e K_{1+}}. \tag{16}$$

In this case n_1/n_+ is proportional to $1/n_e$, a fact observed in Fig. 5(a) as well.

(b) *A region of high* n_e *values above* $n_e \approx 5 \times 10^{22}$ m^{-3}. Collisional excitation and de-excitation processes dominate transport and radiative losses, so that the system will be in local Saha equilibrium (LSE) for which the Saha formula predicts $n_1/n_+ \propto n_e$ dependency as shown in the figure.

(c) *A region of intermediate* n_e *values from* $n_e \approx 5 \times 10^{17}$ m^{-3} *to* $n_e \approx 5 \times 10^{22}$ m^{-3}. In this interval, stepwise collisional processes are much more effective. This will result in a rapid decrease of the deviations of Saha equilibrium (Fig. 5) for increasing n_e values.

To finish this section, the relation between flow through the system, the effective ionization flow and the effective recombination flow is investigated as function of n_e. The relation between the three flows can be written as:

$$\nu_t^+ n_+ = n_e n_1 K_{CR} - n_e n_+ \alpha_{CR}$$

or, expressed in terms of the transport frequency ν_t^+:

$$\nu_t^+ = \frac{n_e n_1 K_{CR}}{n_+}\left(1 - \frac{n_+ \alpha_{CR}}{n_1 K_{CR}}\right). \tag{17}$$

Equation 17 expresses that the ionization flow equals the ion transport flow if the recombination is completely absent. In Fig. 6, factors $n_e n_1 K_{CR}/n_+$ and $n_+ \alpha_{CR}/n_1 K_{CR}$ are plotted as functions of n_e for some ν_t^+ values at $T_e = 0.6$ eV. It appears from this figure that at low and even at intermediate n_e values, the ion transport flow through the system is more or less as large as the effective ionization flow, while the

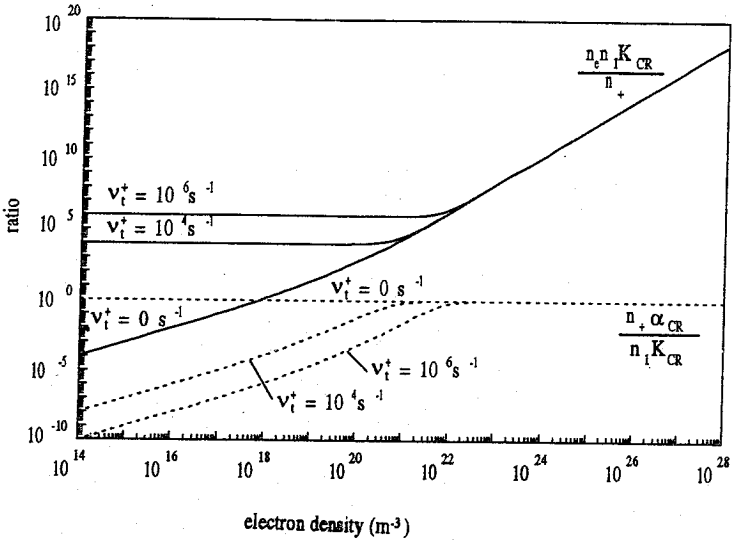

Fig. 6. The factors $n_e n_1 K_{CR}/n_+$ and $n_+ \alpha_{CR}/n_1 K_{CR}$ as a function of n_e at $T_e = 0.6$ eV for some ν_t^+ values for the same conditions as given in Fig. 5.

recombination flow is small compared to the ionization flow for the selected values $\nu_t^+ = 10^4\ s^{-1}$ and $\nu_t^+ = 10^6\ s^{-1}$.

5.2. *Time dependent behaviour*

To simulate the time dependent behaviour of the Li system, we start using the results obtained from the steady state calculations. These give the initial ASDF before the switching off of the EM field. When the EM field is switched off, the field decays to T_h with a time constant $\tau_{EM} = 1.5$ μs [1] and the electron temperature will decay according to:

$$T_e(t) = T_h + (T_e^0 - T_h)\left(\frac{E(t)}{E_0}\right)^2 = T_h + (T_e - T_h)\exp\left(\frac{-t}{\tau_{eh}^\epsilon}\right) \tag{18}$$

where, for the decay time of T_e, τ_{eh}^ϵ yields:

$$\tau_{eh}^\epsilon = \frac{1}{2}\tau_{EM}. \tag{19}$$

The equation can be derived easily from the electron energy equation assuming that the energy coupled into the electrons is directly and completely transferred to the heavy particles. Not only the electron temperature will decay after switching off, but owing to recombination with Ar ions, the electron density will decay with a time constant, τ_{n_e}, in the order of 180 μs [1]. Thus:

$$n_e(t) = n_{e0}\exp\left(\frac{-t}{\tau_{n_e}}\right). \tag{20}$$

At switching on of the generator, T_e and n_e are assumed to restore their original values with the same time constants as given in Eqns 18 and 20.

The changes in T_e will be reflected in α_{CR} and K_{CR}, but not in the evaporation source, because the evaporation does not directly depend on T_e. These facts will cause n_1 and n_+ to change in time, according to Eqns (2) and (4). It is obvious that the densities of the excited levels, which are in QSS with n_1, n_+, n_e and T_e, will also react, simply because the input parameters have changed. Therefore, the response of the Li system can be calculated by the following scheme:

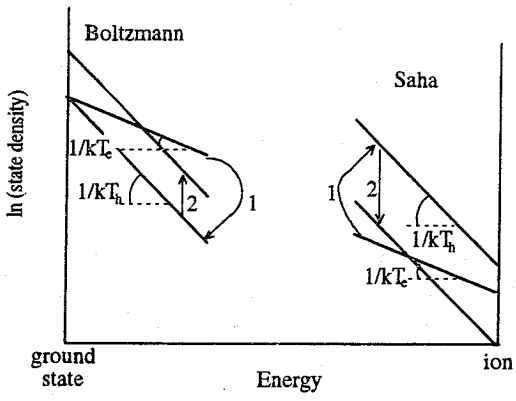

Fig. 7. The response to the power interruption for levels that are ruled by the Boltzmann or Saha balance. Two phenomena are visible. First, the response to electron cooling from T_e to T_h (1). Secondly, recombination of the ions towards the ground level (2).

1. calculate the steady state densities before switching off for a given T_e, n_e, ν_t^+ and S_1^{evap};
2. make a time step of $t = t + \Delta t$;
3. apply models for $T_e(t)$ and $n_e(t)$ as given in Eqns (18) and (20);
4. calculate the densities of excited levels α_{CR} and K_{CR} using the QSS concept and input parameters $n_1(t - \Delta t)$, $n_+(t - \Delta t)$, $n_e(t)$ and $T_e(t)$;
5. calculate $n_1(t)$ and $n_+(t)$ using Eqns (2) and (4); and
6. if the final time is not reached, go back to step 2.

The time steps in our calculations vary typically from 0.1 to 1.0 μs; in the cooling and the heating period, shorter time steps are chosen.

Before showing the results of numerical calculations, we repeat the global explanation as given on the basis of experimental results [2]. Since Li(2*p*) is ruled by the Boltzmann balance of excitation from and de-excitation to the ground level, the density of this level will decrease at switching off due to the cooling of the electrons. This happens at the small time-scale τ_{eh}^{ϵ}. Simultaneously, but at a larger time-scale, ions will recombine to the atomic ground level and consequently, the atomic ground level density will increase. Since the recombination is relatively slow, compared to the change in the Boltzmann balance for the excited level, this effect is observed after the cooling. When $n_1/n_+ \leq 1$, the recombination flow will increase the ground level density significantly (Fig. 7). The bottle-neck in the explanation given in Ref. [2] is that the experiments only give information about the excited levels and not about the main particle reservoirs, the atom ground level or the ionic ground level. The present model does give global information about the main particle reservoirs; so, with the model, we can check the explanation as given in Ref. [2].

The time dependent model is applied for several values of ν_t^+ and T_e, whereas $n_e = 3 \times 10^{20}$ m^{-3} and $\gamma = 1.1$ ($\gamma = T_e/T_h$). The electron decay time, τ_{n_e}, is chosen to be 150 μs. It is further chosen that $S_1^{evap} = 11\nu_t^+ n_+$, which states that under steady state conditions $\nabla\cdot(n_1 w_1) = -\nu_t^+ n_+ + S_1^{evap} = 10\nu_t^+ n_+$. This means physically that most of the evaporated analyte will not ionize but is transported as ground level atoms. This is especially to be expected for lower temperatures. In Fig. 8 the results are shown. First, we will look at the Li(2*p*) level, the level that was investigated intensively during experiments [2]. The calculated Li(2*p*) density shows, in most cases, a downward jump at the switch off, while after the electron cooling the density can increase as well as decrease, depending on the input parameters. At switching on the electric field, the inverse processes occur and the density returns slowly to the value before switching off. Since the calculated responses are all observed experimentally, it seems that all of the models, the separate aurora, the aurora overlap and the transportless model are all applicable and its success depends on the position in the

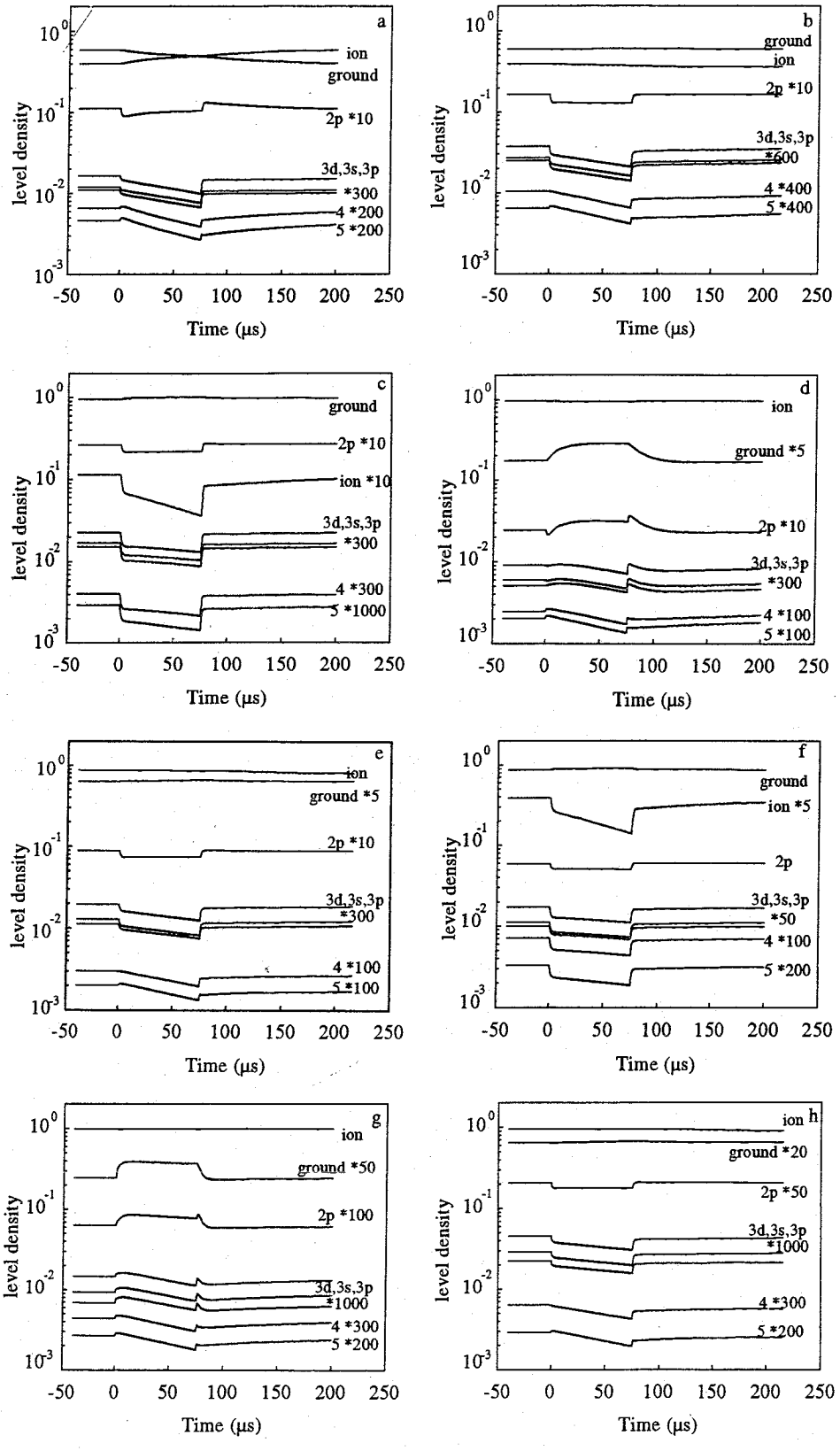
a
ion
ground
2p *10
3d,3s,3p
*300
4 *200
5 *200
b
ground
ion
2p *10
3d,3s,3p
*600
4 *400
5 *400
c
ground
2p *10
ion *10
3d,3s,3p
*300
4 *300
5 *1000
d
ion
ground *5
2p *10
3d,3s,3p
*300
4 *100
5 *100
e
ion
ground *5
2p *10
3d,3s,3p
*300
4 *100
5 *100
f
ground
ion *5
2p
3d,3s,3p
*50
4 *100
5 *200
g
ion
ground *50
2p *100
3d,3s,3p
*1000
4 *300
5 *200
h
ion
ground *20
2p *50
3d,3s,3p
*1000
4 *300
5 *200
level density
Time (μs)

Fig. 8(a)–(h).

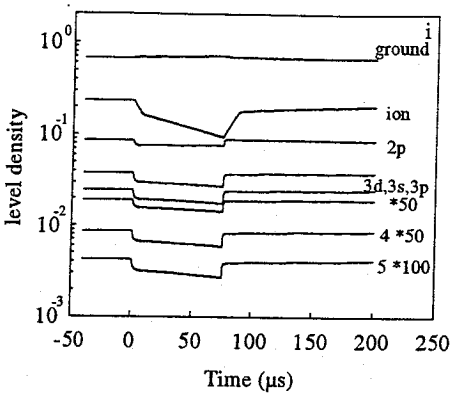

Fig. 8. Calculated responses to power interruption for $n_e = 3 \times 10^{20}$ m^{-3} and $\gamma = 1.1$ during the steady state. At switching off, T_e decays to T_h with a time constant of 0.75 μs and the electrons decay with a time constant of 150 μs. The calculations are performed for T_e = 0.4 eV (a)–(c); 0.5 eV (d)–(f); 0.6 eV (g)–(i); and for $\nu_t^+ = 0$ s^{-1} (a), (d) and (g); 10^4 s^{-1} (b), (e) and (f); and 10^6 s^{-1} (c), (f) and (i).

plasma. Therefore, we need a fluid model that gives additional information about the evaporation and the temperature in the central region as a function of the axial position. This model is the subject for a future study.

The next part in our verification is looking at whether the response of the Li(2*p*) after the cooling of T_e corresponds to the response of the Li(2*s*) (ground) level. It turns out that this is absolutely true. The density of the Li(2*p*) level is completely dominated by the Boltzmann balance of excitation and of de-excitation to the ground level. For the higher excited levels this is not the case, because the Saha balance becomes more important approaching the continuum. Further analysis of the results show that the peaks at switching off and on are, for small ν_t^+ values, caused dominantly by, respectively, a recombination flow and an ionization flow. In the case of large ν_t^+ values, the peak is caused by, respectively, a lack of ionization flow (off switch) and an overshoot in the ionization flow (on switch).

6. Conclusions

To understand the experimental results of the response of Li emission to the power interruption, a time dependent CR model was constructed with an analytical top. An important feature of the model is found to be that the ASDF is sensitive to the outward transport of ions.

To obtain an insight into the order of the ion transport frequency we used a global model. This provides three transport modes.

(a) Transportless model, corresponding to $\nu_t^+ = 0$ s^{-1}; the ASDF is comparable to those obtained by Hasegawa and Haraguchi [5] and Bacri and Gomes [6].

(b) Aurora overlap model, corresponding to $\nu_t^+ = 10^4$ s^{-1}; this is supposed to give a good description at positions where the temperatures are moderate and the gradient lengths around the droplets are so large that the auroras around the droplets overlap each other.

(c) Separate aurora model, corresponding to $\nu_t^+ = 10^6$ s^{-1}; this is supposed to give a good description at positions where the temperatures are high and the gradient lengths around the droplets small, so that the droplets evaporate separately.

Apart from the cases described above, where the transport through the system is caused by production of analyte, there is also the possibility that an increase of T_e causes an ionization flow.

Tests of the CR model on steady state conditions show that the temperature at which the ion density is equal to the ground level density increases with ν_t^+.

The results of the time dependent calculations reveal that the experimentally obtained response to power interruption as presented in Ref. [2] for the first excited level, Li($2p$), can be explained globally. In the lower and the inner parts of the central region, the values of ν_t^+ must be in the order of 10^4 to 10^6 s^{-1}, while in the higher and the outer parts of the central region, small values of ν_t^+ (≈ 0 s^{-1}) can be found. Owing to the fact that the Li($2p$) level is dominated by the Boltzmann balance to the atomic ground level, the Li($2p$) level can be used to monitor the atomic ground level during the power interruption.

References

[1] F. H. A. G. Fey, W. W. Stoffels, J. A. M. van der Mullen, B. van der Sijde and D. C. Schram, *Spetrochim. Acta* **46B**, 885 (1991).
[2] F. H. A. G. Fey, J. M. de Regt, J. A. M. van der Mullen and D. C. Schram, *Spectrochim. Acta* **47B**, 1447 (1992).
[3] J. A. M. van der Mullen, *Phys. Rep.* **191**, 109 (1990).
[4] J. A. M. van der Mullen, *Spetrochim. Acta* **45B**, 1 (1990).
[5] T. Hasegawa and H. Haraguchi, *Anal. Chem.* **59**, 2789 (1987).
[6] J. Bacri and A. M. Gomes, *Spectrochim. Acta* **47B**, 219 (1992).
[7] M. Mitchner and C. H. Kruger, *Partially Ionized Gases*. Wiley, New York (1973).
[8] L. Vriens and A. H. M. Smeets, *Phys. Rev. A* **22**, 940 (1980).
[9] W. L. Wiese, M. W. Smith and B. M. Miles, *Atomic Transition Probabilities*. NBS, Gaithersburg (1969).
[10] D. A. Benoy, J. A. M. van der Mullen and D. C. Schram, *J. Quant. Spectrosc. Radiat. Transfer* **46**, 195 (1991).